Journal of Applied Polymer Science

Synthesis and Properties of Novel Alicyclic-Functionalized Polyimides Prepared from Natural —(D)-Camphor

Hengsheng Zhang, Juan Li, Zhilin Tian, Feng Liu
Department of Chemistry, Nanchang University, Nanchang, Jiangxi 330031, People's Republic of China
Correspondence to: F. Liu (E-mail: liuf@ncu.edu.cn)

ABSTRACT: In this article, a new alicyclic-functionalized diamine, 1,3-bis(4-aminophenoxymethylene)-1,2,2-trimethylclopentane (BAMT) was successfully synthesized starting from natural —(D)-camphor through four reaction steps of oxidation to offer a dicaboxylic acid, reduction to offer a diol, nucleophilic substitution to give a dinitro compound and then reduction to give the final diamine. Two alicyclic-containing polyimides were prepared by polycondensing BAMT with 3,3′,4,4′-biphenyltetracarboxylic dianhydride (BPDA) and 4,4′-oxydiphthalicanhydride (ODPA), respectively. For the studies of the structure–property relationships of the polyimides, one aromatic polyimide of 4, 4'-oxydianiline (ODA) polycondensed with ODPA was prepared in comparison. The alicyclic-containinig polyimides PI (BPDA-BAMT) and PI (ODPA-BAMT) maintain good thermal properties with glass transition temperatures (T_g) of 257°C and 240°C, and temperatures at 5% weight loss (T_5) of 443°C and 436°C in nitrogen, respectively. The alicyclic polyimides exhibit tensile strengths of 91.9–133 MPa, Young's moduli of 2.75—3.24 GPa, and elongations at break of 5.6–18%. Compared with the aromatic polyimide PI (ODPA-ODA), PI (ODPA-BAMT) shows improved transparency with the UV-Vis transmittance at 500 nm over 80%. In addition, PI (ODPA-BAMT) displays better solubility than PI (ODPA-ODA), which has been confirmed by the bigger *d*-spacing value of PI (ODPA-BAMT) than that of PI (ODPA-ODA) calculated from the Wide-angle X-ray Diffraction spectra. This study indicates that the renewable forestry compound, such as natural —(D)-camphor, could be a good origin for the structural designing and preparation of alicyclic-containing polyimides with outstanding combined features suitable for advanced microelectronic and optoelectronic applications. © 2013 Wiley Periodicals, Inc. J. Appl. Polym. Sci. 129: 3333–3340, 2013

KEYWORDS: polyimides; films; thermoplastics

Received 28 November 2012; accepted 20 January 2013; published online 25 February 2013
DOI: 10.1002/app.39053

INTRODUCTION

As a class of high performance polymers, aromatic polyimides with excellent thermal, mechanical, electrical properties, and chemical resistance have been extensively applied in the areas such as aerospace, membrane, microelectronics, and optoelectronics.[1–3] The excellent properties of the aromatic polyimides arise from stiff and ordered polymer chain structure, which was mainly attributed to the inter- and intra-molecular charge transfer (CT) complex formation between the moiety of the diamine (donor) and the moiety of the dianhydride (acceptor). However, CT interaction also brings about some drawbacks for aromatic polyimides including poor processability, high-dielectric constant, and intense coloration (poor transparence), thus limiting the application of aromatic polyimides in some high-tech fields where low dielectric constant of polymer matrices (associated with circuit signal propagation speed in microelectronics) and the absence of color (specially in optoelectronics) are important requirements.[4,5] Therefore, various endeavors of structural modification have been made to suppress the CT interaction of polyimides while maintaining their excellent properties. The modification approaches have included the incorporation of bulky substituents,[6,7] fluorine group,[8–11] flexible linkage,[12,13] twisted or unsymmetrical structures into polymer chain.[14–16] Very recently, much attention has been focused on the introduction of alicyclic structure. The nonaromatic structure in the alicyclic-containing polyimides would disturb the conjugated chain structure and weaken the CT interaction, resulting in the improvement of processability, dielectric properties and alleviated coloration.[17–20] These alicyclic-containing polyimides still retain good thermal stability since an alicyclic structure would impart main chain rigidity and reduce the probability of main chain scission because of the presence of multibonds.[21,22] Currently, the principal methodology of synthesizing alicyclic monomers is by fully hydrogenating their aromatic analogs, which limits the substrate scope of the structural designing and preparation of the alicyclic-containing polyimides.

On the other hand, many natural forestry compounds are structurally characteristic of containing functional alicyclic structures with sufficient reactivity, allowing further structural modification. For instance, natural —(D)-camphor obtained from the cinamomum camphora tree of lauraceae family is an botanical alicyclic hydrocarbon with bicyclo [2, 2, 0] structure and has long been valued for acting as enantiopure precursor or chiral auxiliary mediator in asymmetric synthesis.[23] We envisioned that such natural resource compounds could be excellent abundant library of alicyclic origin for polyimides after being structurally transformed appropriately. In addition, unlike any fossil/petroleum product, there is no fear of ultimate shortage as they are from regenerative, renewable source. Therefore, the exploitations of natural resource compounds with alicyclic structures are worth proceeding as they would add an eco-friendly alternative strategy to the existing methodologies of preparing alicylic polyimides. Herein this research described a pathway of preparing an alicyclic-functionalized diamines from the readily available inexpensive renewable natural —(D)-camphor. The properties of the resultant alicyclic-containing polyimides were comparatively studied in terms of solubility, and the thermal, mechanical, and optical properties.

EXPERIMENTAL

Materials

Natural —(D)-camphor ([α] = +44.30°, m.p.: 179°C), *p*-Chloronitrobenzene (m.p.:81–84°C) and sodium hydride were purchased from Sinopharm Chemical Reagent, China and used as received. Hydrazine hydrate (85%), Pd/C (5%), 4,4′-Oxydianiline (ODA), 4,4′-Oxydiphthalicanhydride (ODPA) and 3,3′,4,4′-Biphenyltetracarboxylic dianhydride (BPDA) were commercially obtained and used as received. *N,N*-Dimethylformamide (DMF) and *N,N*-Dimethylacetylamide (DMAc) were distilled over phosphorus pentoxide. Ether and toluene were distilled over sodium. All other reagents were obtained from various commercial sources and used without further purification.

Measurement

IR spectra were recorded on an Agilent Fourier Transform Infrared spectrometer FTS-40. ^{1}H-NMR spectra were measured on a Bruker DRX 400 spectrometer with DMSO-d_6 or $CDCl_3$ as the solvent and tetramethylsilane as the internal reference. The melting points were determined with a microscopic melting point apparatus SGW-X4 (Shanghai Science Apparatus, China). Optical rotations of the optical active compounds were measured on a polarimeter WXG-4 with the polarized light wavelength of 589 nm at 25°C. The inherent viscosities of the polymers were measured with an Ubbelohed viscometer at 30°C. Wide-angle X-ray diffraction (WAXD) measurement were performed at room temperature (about 25°C) on a Bede XRD Di system, using graphite-monochromatized Cu-Kα radiation (λ = 0.15405 nm). Ultraviolet visible (UV-Vis) spectra of the polymer films were recorded on a Shimadzu UV-visible spectrophotometer UV-2450. Thermogravimetric analysis (TGA) was conducted at a heating rate of 10°C/min under nitrogen flowing on a Perkin-Elmer TGA 2. Dynamic mechanical analysis was conducted with DMA Q800 V20.22 Build 41. An Instron universal tester model 1122 (GB/T1040.1-2006) was used to study the stress–strain behavior of the polyimieds film samples, and the measurement were performed at room temperature with a stretching rate of 5 mm/min.

Monomer Synthesis

The general synthetic route of BAMT starting from natural —(D)-camphor was shown in Scheme 1.

The Synthesis of (1S,3R)-(+)-Cis-1,2,2-trimethylcyclopentane-1,3-dicarboxylic acid (TCDA). A mixture of natural —(D)-camphor 19.0 g (0.125 mol), $FeSO_4{\cdot}7H_2O$ 1.05 g (3.8 mmol), HNO_3 180 mL (65–68%) and 85 mL of water was refluxed at 100–105°C for 3 days, then the resulting solution was cooled to room temperature. The white solid precipitate was collected and washed twice with water to give 12.2 g the desired compound TCDA, yield: 49%, m.p.:181–183°C, [α] = +54.90°.

FTIR (KBr, cm^{-1}), 3419 (O—H stretching); 2976, 2892 (C—H stretching); 1706 (—C=O stretching); 1276 (C—O stretching). ^{1}H-NMR (400 MHz, DMSO-d_6, δ ppm), 0.75 (s, 3H); 1.13 (s, 3H); 1.19 (s, 3H); 1.36 (m, 1H, J = 10 Hz); 1.73 (m, 1H, J = 16 Hz); 1.97 (m, 1H, J = 14 Hz); 2.35 (m, 1H, J = 14 Hz); 2.74 (t, 1H, J = 12 Hz); 12.16 (s, 2H).

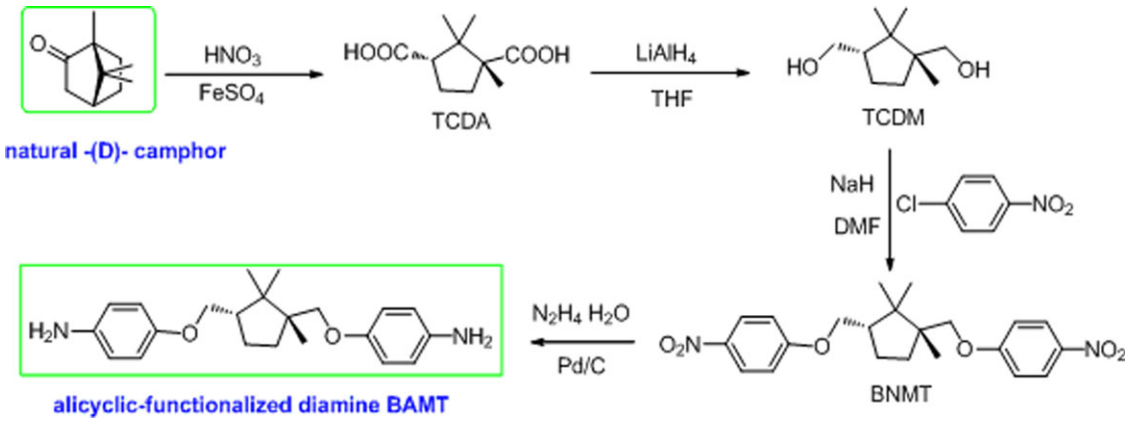

Scheme 1. The general synthetic route of 1,3-bis(4-aminophenoxymethylene)-1,2,2-trimethyclopentane (BAMT). [Color figure can be viewed in the online issue, which is available at wileyonlinelibrary.com.]

The Synthesis of (1S,3R)-(+)-Cis-1,2,2-trimethylcyclopentane-1,3-dimethanol (TCDM)

Lithium aluminum hydride 2.0 g (52.6 mmol) and 30 mL of anhydrous ether were placed in a 250-mL three-necked flask equipped with a reflux condenser. Then in an ice bath (10°C), a solution of 3.0 g (15 mmol) TCDA in 40 mL THF was added dropwise by a constant pressure funnel over 1 h. The ice bath was then removed and the mixture was stirred for 5 h at room temperature. The redundant lithium aluminum hydride was carefully quenched with 8.5 g $Na_2SO_4{\cdot}10H_2O$, then the white slurry was filtered, extracted with 50 mL CH_2Cl_2 and dried over Na_2SO_4, and concentrated under vacuum to give the crude product, which was recrystallized with CH_2Cl_2/n-haxane (v/v 1:1) to offer 1.8 g white crystalline solid (+)-cis-1,2,2-trimethylcyclopentane-1,3-dimethanol (TCDM), yield:71%, m.p.:137–139°C, $[\alpha] = +41.85°$.

FTIR (KBr, cm^{-1}), 3355 (O—H stretching); 2958, 2875 (C—H stretching); 1235 (C—O stretching). ^{1}H-NMR (400 MHz, $CDCl_3$, δ ppm), 0.80 (s, 3H); 1.04 (s, 6H); 1.62 (m, 1H, $J = 32$ Hz); 1.97 (m, 2H, $J = 12$ Hz); 2.12 (m, 2H, $J = 12$ Hz); 3.49 (m, 2H, $J = 14$ Hz); 3.53 (m, 2H, $J = 4$ Hz); 3.61 (m, 1H, $J = 14$ Hz); 3.75 (m, 1H, $J = 10$ Hz).

The Synthesis of (1S,3R)-(+)-1,3-bis(4-nitrophenoxy-methylene)-1,2,2-trimethylcyclopentane (BNMT)

In a 100-mL dry three-necked round-bottom flask, 0.34 g (14.1 mmol) NaH and 1.2 g (7.05 mmol) TCDM in 5 mL DMF were stirred for 3 h at 50°C. Then 2.01 g (14.1 mmol) *p*-chloronitrobenzene in 7 mL DMF was added dropwise and stirred at room temperature overnight. The mixture was poured into 500 mL distilled water, and the precipitated was washed with ethanol twice and recrystallized with DMF to give 1.2 g (1S,3R)-(+)-1,3-bis(4-nitrophenoxymethylene)-1,2,2-trimethylcyclopentane (BNMT) as yellow crystalline solid, yield: 40%, m. p.: 155–157°C, $[\alpha] = +53.00°$.

FTIR (KBr, cm^{-1}), 3083 (Ar—H stretching); 2958, 2863 (C—H stretching); 1501, 1335 (C—N stretching); 1262 (C—O stretching). ^{1}H-NMR(400 MHz, $CDCl_3$, δ ppm), 8.21 (m, 4H, $J = 12$ Hz); 6.94 (m, 4H, $J = 4$ Hz); 3.85–4.13 (m, 4H, $J = 56$ Hz); 2.48 (t, 1H, $J = 10$ Hz); 1.53–2.11 (m, 4H, $J = 116$ Hz); 1.21 (s, 6H); 0.89 (s, 3H).

Elemental analysis ($C_{22}H_{26}N_2O_6$): Calcd. C 63.76, H 6.32, N 6.76; found C 63.84, H 6.53, N 6.89.

The Synthesis of (1S,3R)-(+)-1,3-bis(4-aminophenoxy-methylene)-1,2,2-trimethyclopentane (BAMT)

A mixture of 1.0 g (2.6 mmol) BNMT, 0.1 g Pd/C and 16 mL absolute alcohol was placed in a 100-mL three-necked flask equipped with a reflux condenser and a dropping funnel. The mixture was kept refluxing for 30 min, then 6 mL hydrazine hydrate was added dropwise and the reaction mixture was refluxed for 8 h. The resultant reaction mixture was filtered while hot to remove Pd/C, and the filtrate was then concentrated under vacuum to give the crude product, which was purified by recrystallization with ethanol/water to give 0.85 g off-white solid BAMT, yield 90%, m.p.: 117–119°C, $[\alpha] = +45.15°$.

FTIR (KBr, cm^{-1}), 3421, 3342 (N—H stretching); 3013 (Ar—H stretching); 2963, 2867 (C—H stretching); 1228 (C—O stretching). ^{1}H-NMR(400 MHz, $CDCl_3$, δ ppm), 6.73 (m, 4H, $J = 10$ Hz); 6.63 (m, 4H, $J = 6$ Hz); 3.65–3.93 (m, 4H, $J = 56$ Hz); 3.35 (s, 2H); 2.34 (t, 1H, $J = 10$ Hz); 1.45–2.03 (m, 4H, $J = 116$ Hz); 1.11 (s, 6H); 0.82 (s, 3H).

Elemental analysis ($C_{22}H_{30}N_2O_2$): Calcd. C 74.54, H 8.53, N 7.90; found C 74.93, H 8.75, N 8.11.

Polymer Synthesis

The typical two-step method was adopted to prepare the objective polyimides. A general polymerization procedure could be illustrated by the following example. 0.6000 g (1.692 mmol) of BAMT was placed in 10 mL DMAc in a 100-mL three-necked flask fitted with a nitrogen inlet and stirred until complete dissolution. Then 0.5218 g (1.692 mmol) of ODPA was added and the mixture was stirred for 12 h at room temperature to yield a viscous poly (amic acid) (PAA) solution. The obtained PAA was cast onto a clean glass plate, followed by thermally curing with a programmed procedure of 100°C/1 h, 150°C/1 h, 200°C/1 h, 250°C/2 h to produce the fully imidized polyimide film PI(ODPA-BAMT). The structure of the polyimides synthesized and studied in this article was shown in Scheme 2.

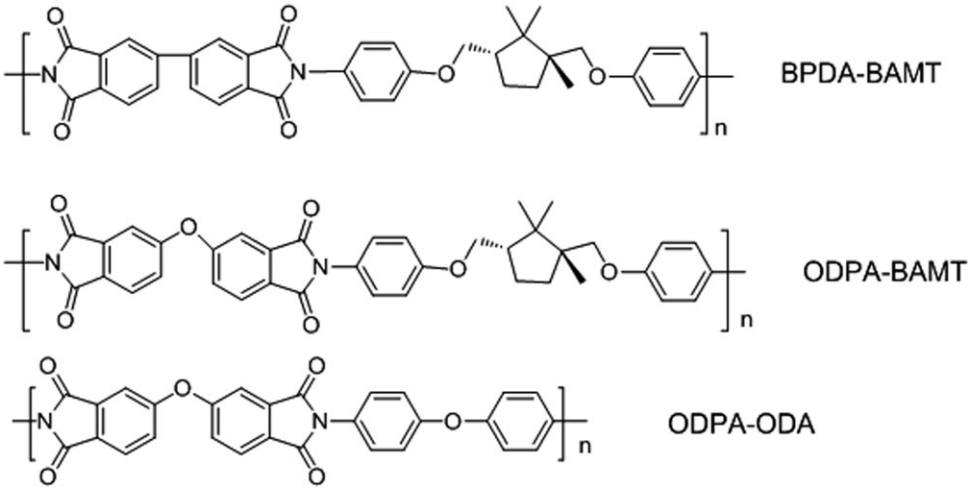

Scheme 2. The structure of the three polyimides.

Applied Polymer SCIENCE

RESULTS AND DISCUSSION

Monomer Synthesis

As shown in Scheme 1, the novel alicyclic-functionalized diamine monomer BAMT was synthesized starting from natural —(D)-camphor via oxidation to offer dicarboxlic acid, followed by reduction to give diol, and then Williamson reaction to produce the ether-linked alicyclic-functionalized dinitro compound, and reduction by hydrazine hydrate to give the final diamine. The ^{1}H-NMR spectra of TCDA (DMSO-d_6 as solvent) and TCDM ($CDCl_3$ as solvent) were shown in the Figures 1 and 2, respectively. The signal of carboxylic protons (H_1 and H_6) of TCDA at 12.16 ppm disappeared and the signals of hydroxyl protons (H_1 and H_7) of TCDM were observed in Figure 2, which confirmed that the reduction of carboxyl group into hydroxyl group was effectively carried out. The ^{1}H-NMR and FTIR spectra of BNMT and BAMT were also shown and the peaks were also structurally assigned in Figures 3 and 4, respectively. The ^{1}H-NMR signals of different aromatic protons in BNMT show an obvious shift divergence, which is attributed to the strong electron-withdrawing effect of the attached nitro substituents. In comparison, owing to the mild electron-donating effect of attached amino substituents, the signals of different aromatic protons in BAMT do not display appreciable shift divergence, and the proton absorption of amino in BAMT could be observed in the ^{1}H-NMR spectra. In FTIR spectra, the characteristic absorption of nitro group in BNMT and amino group in BAMT are observed in 1335 and 1501 cm^{-1}, and 3342 and 3421 cm^{-1}, respectively.

Polymer Synthesis

The three polyimides PI (ODPA-BAMT), PI (BPDA-BAMT), and PI (ODPA-ODA) were prepared by polycondensation through a two-step imidization procedure. The chemical structures of the polyimides were characterized by FTIR. As shown in Figure 5, both the polyimides show the characteristic imide absorption bands at around 1777 cm^{-1}, 1726 cm^{-1}, and 1383 cm^{-1}, which were attributed to the asymmetrical carbonyl stretching vibrations, the symmetrical carbonyl stretching vibrations and C—N stretching, respectively. The absorptions around 2965 cm^{-1} and 2887 cm^{-1} of PI (BPDA-BAMT) should be assigned to the C—H vibrations of 1, 2, 2-trimethyl substituents in the alicyclic segments.

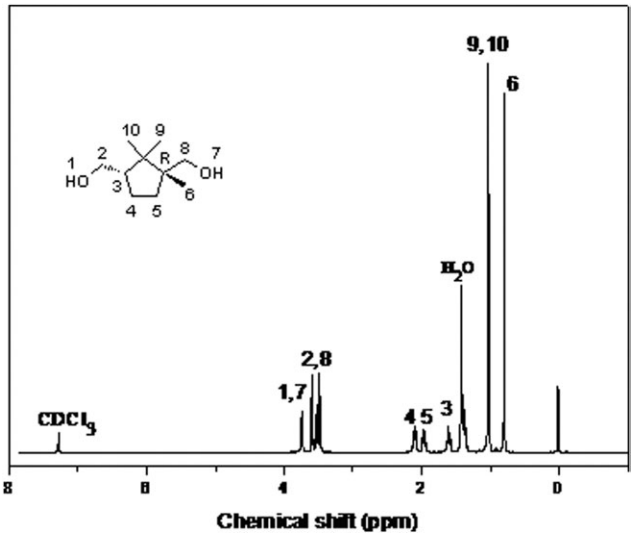

Figure 2. ^{1}H-NMR spectrum of TCDM.

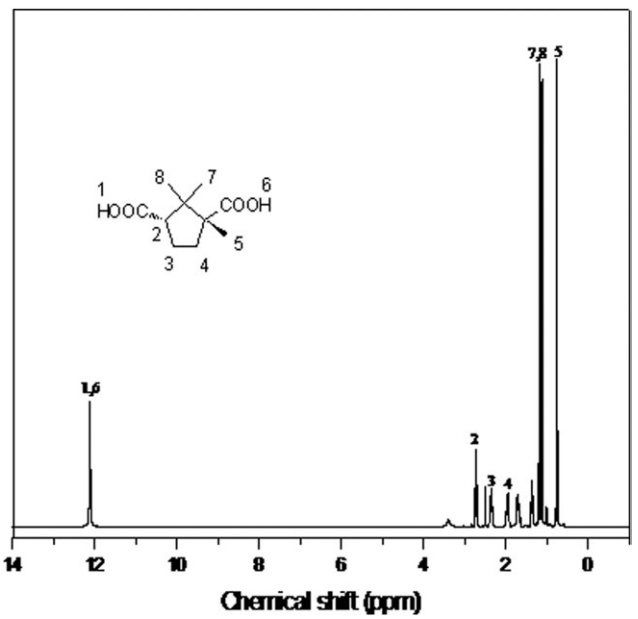

Figure 1. ^{1}H-NMR spectrum of TCDA.

Mechanical and Optical Properties of the Polyimides

For all these polyimide films, the tensile strength varies in the range of 91.9–141 MPa, the elongation at break 5.6–18%, and the initial modulus 2.75–3.44 GPa, as shown in Table I. The alicyclic-containing polyimides PI (BPDA-BAMT) and PI (ODPA-BAMT) show comparable mechanical properties with the

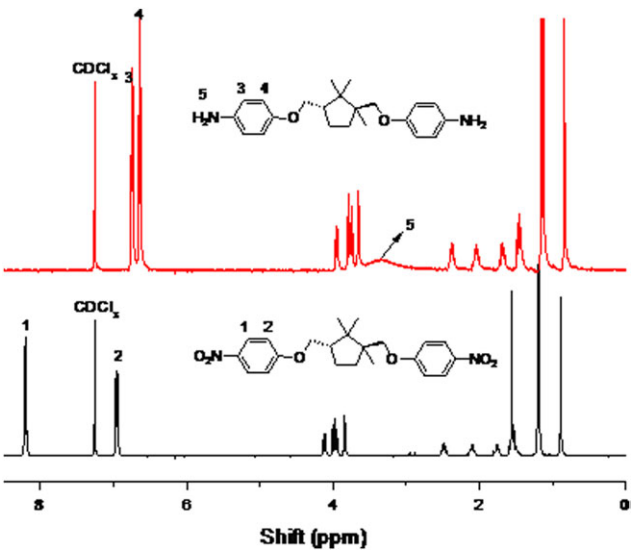

Figure 3. ^{1}H-NMR spectra of BNMT and BAMT. [Color figure can be viewed in the online issue, which is available at wileyonlinelibrary.com.]

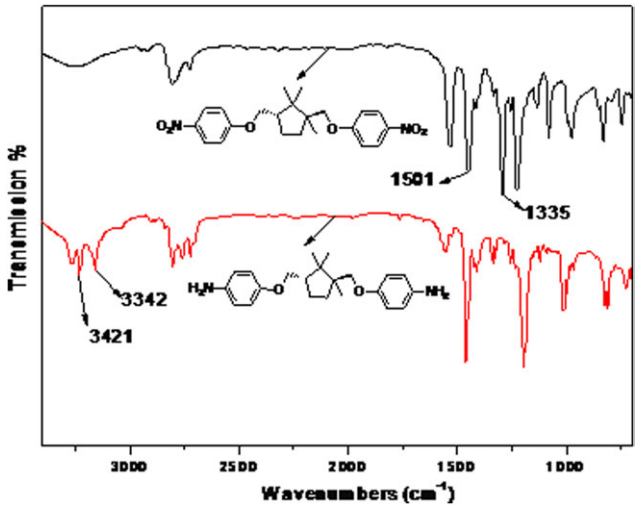

Figure 4. FTIR spectra of BNMT and BAMT. [Color figure can be viewed in the online issue, which is available at wileyonlinelibrary.com.]

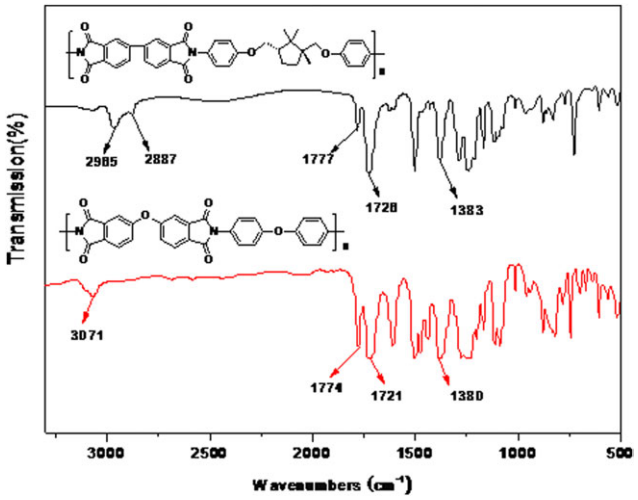

Figure 5. FTIR spectra of the polyimides. [Color figure can be viewed in the online issue, which is available at wileyonlinelibrary.com.]

aromatic polyimide PI (ODPA-ODA). It indicates that the incorporation of the alicyclic 1, 2, 2-trimethyclopentane groups does not bring down but retained the good mechanical properties of the synthesized polyimides.

The UV–Vis spectra of the polyimides films are shown in Figure 6. The cutoff wavelengths range from 380 to 420 nm and the transmittances in the visible region are in 80–90%. The transmittances of the polyimide films at 500 nm were over 70%. The wavelengths at absorption edge (λ_{cutoff}) and the transmittance at 500 nm from the UV–Vis spectra are summarized in Table I. Compared with BPDA-derive polyimide, polyimide films derived by ODPA are fairly transparent and almost colorless. This behavior should be related to the flexible ether linkage in the structure of monomer ODPA that leads to the inhibition of the intermolecular charge-transfer complex (CTC). The PI (ODPA-BAMT) shows the highest transparence with transmittance of 75% at 450 nm, followed by PI (ODPA-ODA) the transmittance of 63%, and the PI (BPDA-BAMT) exhibits the lowest transparence with transmittance of 28%. The higher transparence of PI (ODPA-BAMT) than PI (ODPA-ODA) may mainly be attributed to the weakened conjugation and suppressed CT interaction. The noncoplanar bulky alicyclic-functionalized groups in the diamine (BAMT) moieties in the polymer chain are presumably effective to break the conjugation along the backbone and to decrease the CT formation, thus providing enhanced optical transparency.

Thermal Properties of the Polyimides

The thermal properties of the polyimides were evaluated by means of thermogravimetry analysis (TGA) and dynamic mechanical analysis (DMA), and the results are summarized in Table I. It is shown that for the PI (ODPA-BAMT) and PI (BPDA-BAMT), the onset decomposition temperatures (T_d) are ranged in 416–437°C, about 53–74°C, lower than that of the PI (ODPA-ODA). The PI (ODPA-BAMT) and PI (BPDA-BAMT) exhibit the temperature at 5% weight loss (T_5) and 10% weight loss (T_{10}) values of 436–443°C and 451–463°C, appreciably lower than 528°C and 550°C of aromatic PI (ODPA-ODA),

Table I. Viscosity, Mechanical, Optical, and Thermal Properties of the Polyimides

		Mechanical and optical properties					Thermal properties				
Polyimides	η^a(dL/g)	$E_b{}^b$ (%)	$\sigma_m{}^c$ (MPa)	$E_t{}^d$ (GPa)	$T_{500}{}^e$ (%)	$\lambda_0{}^f$ (nm)	$T_g{}^g$ (°C)	$T_d{}^h$ (°C)	$T_5{}^i$ (°C)	T_{10} (°C)	Char^k (%)
BPDA-BAMT	0.75	18	133	3.24	75	425	257	437	443	463	35
ODPA-BAMT	0.64	5.6	91.9	2.75	80	378	240	416	436	451	25
ODPA-ODA	0.82	12	141	3.44	78	398	271	490	528	550	55

[a]Measured at a concentration of 0.5 g/dL poly(amic acid)s in DMAc at 30°C.
[b]Elongation at break.
[c]Tensile strength.
[d]Tensile modulus.
[e]Transmittance at 500 nm.
[f]UV cutoff wavelength.
[g]Glass transition temperature determined by loss factor curves in DMA results.
[h]Onset decomposition temperature.
[i]Temperature at 5 and 10% weight loss at a 20°C/min heating rate under N_2.
[k]Residual weight percentage at 800°C in N_2.

Applied Polymer SCIENCE

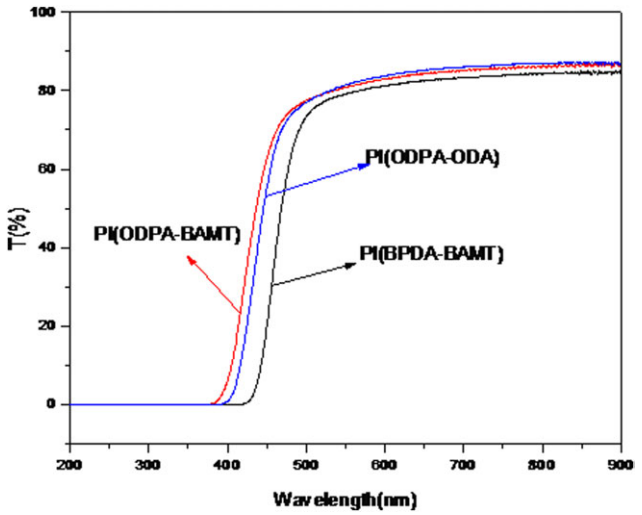

Figure 6. UV-visible spectra of the polyimides. [Color figure can be viewed in the online issue, which is available at wileyonlinelibrary.com.]

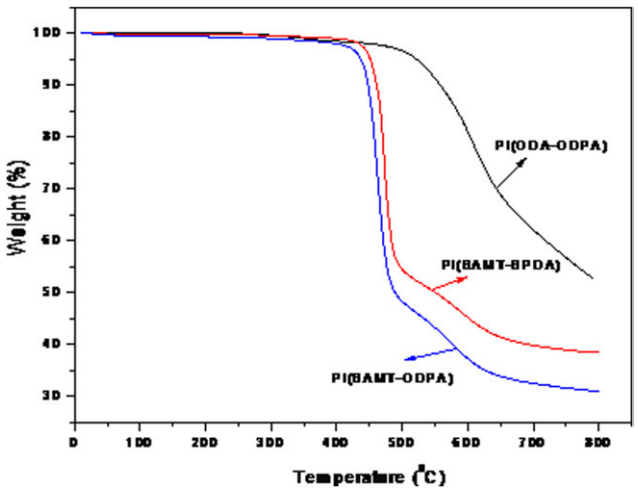

Figure 7. TGA curves of the polyimides. [Color figure can be viewed in the online issue, which is available at wileyonlinelibrary.com.]

respectively. This indicates that the introduction of alicyclic structure would decrease the thermal property of the polyimides in a degree. Still, the alicyclic-containing polyimides PI (ODPA-BAMT) and PI (BPDA-BAMT) exhibit good thermal stability, showing no weight loss below 410°C and char yield of more than 30% in nitrogen. Similarly, both the two alicyclic-containing polyimides show double-stage decomposition processes in nitrogen, as shown in Figure 7. The first degradation stage begins at around 450°C, which could be due to the decomposition of the aliphatic segments. The second stage of the degradation begins at about 500°C, which could be mainly because of the decomposition of the imide structures and aromatic moieties, as also depicted by the TGA curve of PI (ODPA-ODA).

Figure 8 shows the dynamic storage modulus (E'), loss modulus (E'') and loss factor (tanδ) curves as a function of temperature for all the polyimides. It is noted that the loss modulus curves of PI (BPDA-BAMT) and PI (ODPA-BAMT) show two relaxations, one located around 80°C and the other in the range of 225–270°C. The high temperature peak originates from the glass relaxation occurring in the polyimides, and the low temperature peak may originate from the β subglass relaxation.[24] The bulky substituted alicyclic structure would create steric hindrance, thus inhibiting the mobility of the polymer chain. The β

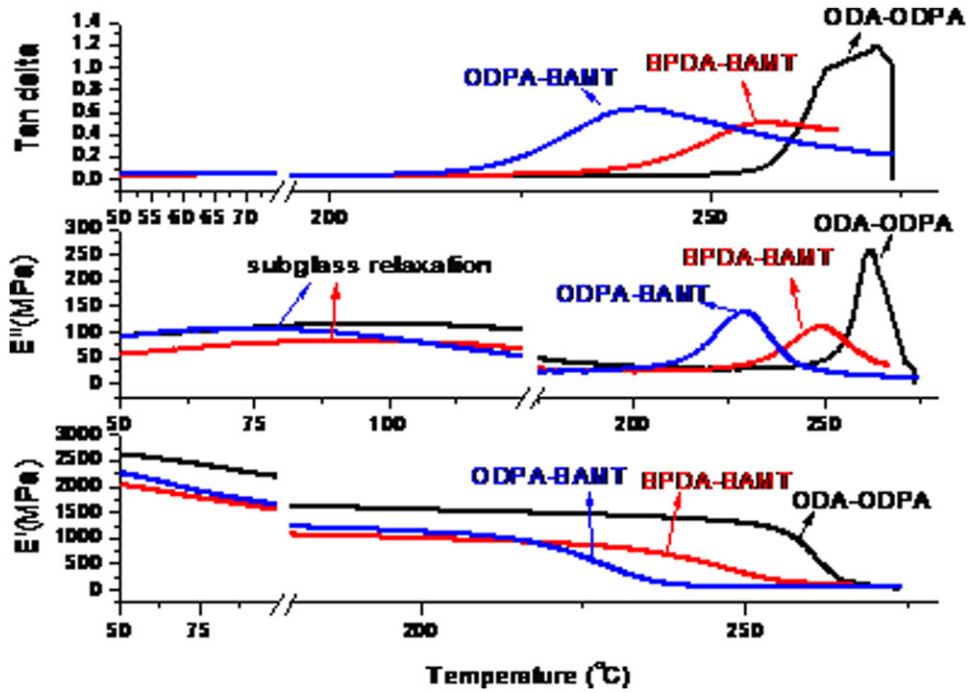

Figure 8. DMA curves of the polyimides. [Color figure can be viewed in the online issue, which is available at wileyonlinelibrary.com.]

Table II. The Solubility and *d*-Spacing of the Polyimides

Polyimides	Solubility[a]							2θ[b] (°)	*d*-Spacing[c] (Å)
	DMF	DMAc	NMP	*m*-Cresol	THF	$CHCl_3$	DMSO		
BPDA-BAMT	—	—	+	—	—	—	—	16.69	5.31
ODPA-BAMT	+	+	++	+	+	—	+	15.79	5.61
ODPA-ODA	—	—	+	—	—	—	—	17.79	4.98

[a]++: soluble at 25°C, +: soluble on heating, —: insoluble on heating.
[b]Measured by WAXD.
[c]Calculated according to Bragg's equation: $2d \sin\theta = n\lambda$, where n is 1 and λ adopts the value of 1.54 Å.

subglass relaxation of the BAMT-derived alicyclic-containing polyimides was presumably assigned to the rotation or oscillation of the three methyl substituents attached to the cyclopentyl ring in the diamine moiety of the polyimides. Seen from the tanδ curves, the PI (BPDA-BAMT) and PI (ODPA-BAMT) showed the glass transition temperature (T_g) at 257°C and 240°C, expectedly lower than 271°C of the T_g of the aromatic polyimide PI (ODPA-ODA).

The Solubility and *d*-Spacing of the Resulting Polyimides

The solubility of the polyimides was tested in various solvents and the results are summarized in Table II, which shows that the solubility of the polyimides depends on the dianhydride structure and the diamine structure as well.[25–28] The effect of the dianhydride structure to the solubility of the polyimides could be comparatively investigated between PI (BPDA-BAMT) and PI (ODPA-BAMT), and it is found that that ODPA containing a flexible ether linkage between two phenyl ring leads to better solubility than BPDA with rigid biphenyl structure does. Similarly, by comparison of the solubility of PI (ODPA-BAMT) with that of PI (ODPA-ODA), it can be found that the alicyclic-funtionalized diamine BAMT containing 1, 2, 2-trimethylcyclopentane groups and ether linkages leads to better solubility than the aromatic diamine ODA with ether-linked aromatic structure does. The better solubility of PI (ODPA-BAMT) may be explained by the disrupted CT interaction of polymer chains by the bulky alicyclic groups in BAMT moieties. Further determination of the polymer chain interaction was carried out by WAXD measurement. As shown in Figure 9, the WAXD patterns of the polyimides show similar, relatively broad peaks, indicating that the polyimides were almost amorphous with only little crystallinity.[29] The most prominent WAXD peak in the amorphous glassy polymer spectra is often used to estimate the average interchain spacing distance (*d*-spacing) according to Bragg's equation.[30] The *d*-spacing values calculated from 2θ follows the relationship PI (ODPA-BAMT)>PI (BPDA-BAMT)>PI (ODPA-ODA), which is in accordance of the solubility order of the polyimides. It indicates that the alicyclic-functionalized BAMT shows significant impact on improving the solubility by enlarging the average polymer interchain distance and thus facilitating the solvation process. Therefore, the introduction of the bulky alicyclic 1, 2, 2-trimethylcyclopentyl group induces loose chain packing and remarkably contributes to the decreased intra- and intermolecular CT interaction, resulting in increased solubility of the synthesized polyimides.

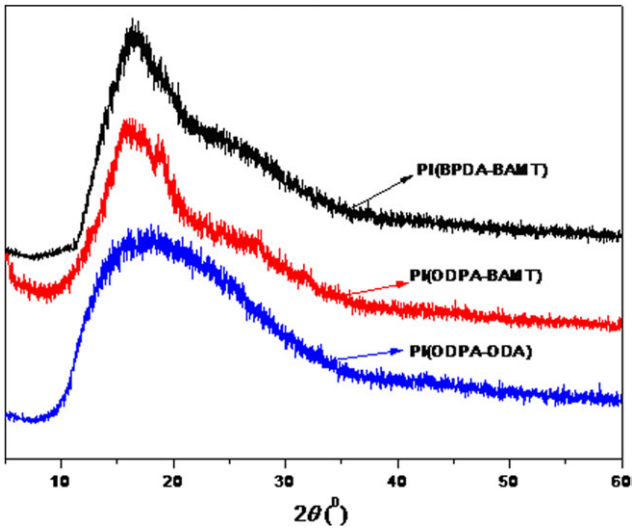

Figure 9. Wide angle X-ray diffraction patterns of the polyimides. [Color figure can be viewed in the online issue, which is available at wileyonlinelibrary.com.]

CONCLUSIONS

A novel alicyclic-functionalized diamine monomer BAMT containing the unsymmetrical 1, 2, 2-trimethyclopentane group was successfully synthesized starting from an readily available inexpensive renewable forestry compound natural —(D)-camphor. The incorporation of the 1, 2, 2-trimethylcyclopentane groups and ether links into the backbone of the polyimides not only improves the solubility and optical transparency but also retains the good mechanical properties and thermal stability, which are desirable for practical applications as engineering plastics, microelectronics and optoelectronics. It indicates that the structural transformation of natural alicyclic-containing forestry compounds would be a promising strategy for designing and preparation of polyimides with the improved practical properties.

ACKNOWLEDGMENTS

Financial support by National Natural Science Foundation of china (Nos. 51263014 and 50803026) and Jiangxi Provincial Council of Science and Technology, China (No. 2009BGA00300) is gratefully acknowledged.

REFERENCES

1. Ding, M. X. *Prog. Polym. Sci.* **2007**, *32*, 623.
2. Liu, Y.; Zhang, Y. H.; Guan, S. W.; Li, L.; Jiang Z. H. *Polymer* **2008**, *49*, 5439.
3. Kim, I. T.; Lee, S. W.; Kwak, T. H.; Lee, J. Y.; Park H. S., Elsenbaumer R. L. *Polym. Prepr. (Am. Chem. Soc., Div. Polym. Chem.)* **2001**, *42*, 415.
4. Kong, C. L.; Zhang, Q. H.; Gu, X. F.; Chen, D. J. *J. Macro. Sci. A: Pure Appl. Chem.* **2006**, *43*, 1825.
5. Chen, C. F.; Qin, W. M.; Huang, X. A. *J. Macromol. Sci. Phys. B.* **2008**, *47*, 109.
6. Matsumoto, T.; Nishimura, K.; Kurosaki, T. *Eur. Polym. J.* **1999**, *35*, 1529.
7. Yang, C. P.; Su, Y. Y.; Hsiao, F. Z. *Polymer* **2004**, *45*, 7529.
8. Hu, T. J.; Wang, C. Q.; Li, F. M.; Harris, F. W.; Cheng, S. Z. D.; Wu, C. *J Polym. Sci. Part B: Polym. Phys.* **2000**, *38*, 2077.
9. Myung, B. Y.; Ahn, C. J.; Yoon, T. H. *Polymer* **2004**, *45*, 3185.
10. Choi, J. K.; Cho, K.; Yoon, T. H. *Synthetic Met.* **2010**, *160*, 1938.
11. Kim, G.; Basarir, F.; Yoon T. H. *Synthetic Met.* **2011**, *161*, 2092.
12. Shao, Y.; Li, Y. F.; Zhao, X.; Ma, T.; Gong, C. L.; Yang, F. C. *Eur. Polym. J.* **2007**, *43*, 4389.
13. Kumar, S. V.; Yu, H. C.; Choi, J.; Kudo, K.; Jang, Y. H.; Chung, C. M., *J. Polym. Res.* **2011**, *18*, 1111.
14. In, I.; Kim, S. Y. *Polymer* **2006**, *47*, 547.
15. Cheng, L.; Jian, X. G.; Mao, S. Z. *J Polym. Sci. Part A: Polym. Chem.* **2002**, *40*,3489.
16. Pal, R.; Patil, P. S.; Salunkhe, M.; Maldar, N.; Wadgaonkar, P. *Eur. Polym. J.* **2009**, *45*, 953.
17. Watanabe, Y.; Sakai, Y.; Shibasaki, Y.; Ando, S.; Ueda, M.; Oishi, Y.; Mori, K. *Macromolecules* **2002**, *35*, 2277.
18. Chern, Y. T.; Shiue, H. C. *Macromol. Chem. Phys.* **1998**, *199*, 963.
19. Kim, E. H.; Moon, I. K.; Kim, H. K.; Lee, M. H.; Han, S. G.; Yi, M. H.; Choi, K. Y. *Polymer* **1999**, *40*, 6157.
20. Oishi, Y.; Onodera, S.; Oravec, J.; Mori, K.; Ando, S.; Terui, Y.; Maeda, K. *J. Photopolym. Sci. Technol.* **2003**, *16*, 263.
21. Havva, Y.; Mathias, L. J. *Polymer* **1998**, *39*, 3779.
22. Chern, Y. T.; Shiue, H. C. *Macromolecules* **1997**, *30*, 4646.
23. Luo, Y. C.; Zhang, H. H.; Wang, Y.; Xu, P. F. *Accounts Chem. Res.* **2010**, *43*, 1317.
24. Artiaga, R.; Chipara, M.; Stephens, C. P.; Benson, R. S. *Nucl. Instrum. Meth. B.* **2005**, *236*, 432.
25. Matsumoto, T. *Macromolecules* **1999**, *32*, 4933.
26. Yang, F. C.; Zhao, J. J.; Li, Y. F.; Zhang, S. J.; Shao, Y.; Shao, H.; Ma, T.; Gong, C. L. *Eur. Polym. J.* **2009**, *45*, 2053.
27. Zhao, X.; Li, Y. F.; Zhang, S. J.; Shao, Y.; Wang, X. L. *Polymer* **2007**, *48*, 5241.
28. Li, H. S.; Liu, J. G.; Wang, K.; Fan, L.; Yang, S. Y. *Polymer* **2006**, *47*, 1443.
29. Qiu, Z. M.; Wang, J. H.; Zhang, Q. Y.; Zhang, S. B.; Ding, M. X.; Gao, L. X. *Polymer* **2006**, *47*, 8444.
30. Niyogi, S.; Adhikari, B. *Eur. Polym. J.* **2002**, *38*, 1237.